

## Low-frequency internal friction study of oxide-ion conductor $\text{La}_2\text{Mo}_2\text{O}_9$

This article has been downloaded from IOPscience. Please scroll down to see the full text article.

2001 J. Phys.: Condens. Matter 13 1641

(<http://iopscience.iop.org/0953-8984/13/8/303>)

View [the table of contents for this issue](#), or go to the [journal homepage](#) for more

Download details:

IP Address: 171.66.16.226

The article was downloaded on 16/05/2010 at 08:42

Please note that [terms and conditions apply](#).

# Low-frequency internal friction study of oxide-ion conductor $\text{La}_2\text{Mo}_2\text{O}_9$

X P Wang and Q F Fang

Laboratory of Internal Friction and Defects in Solids, Institute of Solid State Physics, Chinese Academy of Sciences, Hefei 230031, People's Republic of China

Received 22 November 2000, in final form 12 January 2001

## Abstract

The internal friction of oxide-ion conductor  $\text{La}_2\text{Mo}_2\text{O}_9$  has been measured using a computer-controlled torsion pendulum. Two internal friction peaks were observed around 380 K and 833 K respectively at a vibration frequency of 1 Hz and a heating rate of  $5 \text{ K min}^{-1}$ . The lower-temperature peak is of relaxation type and actually composed of two sub-peaks that originate from the disorder diffusion of two different kinds of oxygen ion in  $\text{La}_2\text{Mo}_2\text{O}_9$ . The relaxation strength of the high-temperature component of this peak is much larger than that of the low-temperature component, which can be understood due to the different concentration of the two kinds of oxygen ion. As for the high-temperature peak at 833 K, it is associated with a first-order phase transition and corresponds to an order–disorder transition in aspects of oxygen ions. Substituting the  $\text{La}^{3+}$  cation to some degree with divalent  $\text{Ca}^{2+}$  can suppress this phase transition and maintain the high-temperature phase to lower temperature.

## 1. Introduction

Oxide-ion conductors have been widely studied because of their potential applications as components of fuel cells, oxygen sensors, oxygen pumps and oxygen-permeable membrane catalysts [1, 2]. Up to now however, only a small number of structural families, such as fluorite, perovskite, inter-growth perovskite/ $\text{Bi}_2\text{O}_3$  layers and pyrochlore [1–4], are suitable for use as oxide electrolytes in consideration of the limitation of operating temperature and conductivity. Recently, Lacorre *et al* [5, 6] reported that lanthanum molybdate  $\text{La}_2\text{Mo}_2\text{O}_9$  exhibits an ionic conductivity as high as  $6 \times 10^{-2} \text{ S cm}^{-1}$  at 1073 K. This compound and its relatives deduced by cationic substitutions have a cubic structure and a different formation mechanism of oxygen vacancy from all other known oxide electrolytes mentioned above. The studies of this kind of compound have opened a new window to the research field of oxide-ion conductors.

The high-temperature form of  $\text{La}_2\text{Mo}_2\text{O}_9$  ( $\beta$ ) belongs to the space group  $P213$ , the same as  $\beta\text{-SnWO}_4$ . The formation mechanism of the intrinsic oxygen vacancy in  $\beta\text{-La}_2\text{Mo}_2\text{O}_9$  can be understood also by comparing with  $\beta\text{-SnWO}_4$ . In  $\beta\text{-SnWO}_4$ , the  $5s^2$  electrons of  $\text{Sn}^{2+}$  are a lone pair, which usually occupied a volume similar to that of an  $\text{O}^{2-}$  anion. Therefore the stoichiometry can be reformulated as  $\text{SnMO}_4\text{L}$ , or  $\text{Sn}_2\text{M}_2\text{O}_8\text{L}_2$ , where L represents a lone pair. Substituting  $\text{Sn}^{2+}$  by  $\text{La}^{3+}$ , a cation of approximately the same size but without a lone pair, will

create two vacancies, one of them being occupied by the extra oxygen that compensates for the cationic valence increase ( $L_2 \rightarrow V+O$ ). The new formula thus becomes  $La_2M_2O_{8+1}V$ , where  $V$  represents the extra vacancy. In addition, the  $La_2Mo_2O_9$  undergoes a slight structural transition around 850 K, resulting in a decrease in conductivity by almost two orders of magnitude at low temperatures [5, 6]. Substituting the  $La^{3+}$  cation with divalent ions such as Ca, Ba etc can suppress this phase transition and maintain the high-temperature phase to lower temperature.

The internal friction (IF) method is a very useful technique for studying the defect structure, ion diffusion mechanism and structural transition in ceramic oxides such as YBaCuO superconductors, doped  $CeO_2$  oxygen ion conductor and so on [7–9]. In this investigation, the low-frequency IF method was used to study the kinetic parameters for the motion of defects and the phase transition characters of the oxide-ion conductor  $La_2Mo_2O_9$ . In section 2, the preparation process of the samples and the apparatus used in this study are described. The experimental results are illustrated in section 3, where two internal friction peaks are discussed separately. Finally the results are discussed and concluded in section 4.

## 2. Experimental details

The ceramic samples of  $La_2Mo_2O_9$  in our experiment were prepared by conventional solid-state reaction from a stoichiometric mixture of  $La_2O_3$  and  $MoO_3$  powders. The well mixed powders were calcined in an alumina crucible at 823 K for 10 hours in air, and then were finely ground and pressed into a mould to form bar samples ( $64 \times 4 \times 1.5 \text{ mm}^3$ ) for the IF measurements. These bar samples were finally sintered at 1223 K for 12 hours in air. In order to obtain much more meaningful experimental results, all samples were made in the same procedure and sintered in the same environmental condition.

Low-frequency IF measurement was made on a computer-controlled torsion pendulum. In order not to change the specimen's state in the measurement of activation energy, the IF was measured with the forced vibration method in which the measurements at different frequencies were carried out by varying the driven frequency in one measurement run. The maximum torsion strain amplitudes were kept at  $2.5 \times 10^{-5}$  in all measurements. Differential scanning calorimetry (DSC) measurements were carried out using a DSC-IIC made by Perkin–Elmer Corporation in the USA. The weight of  $La_2Mo_2O_9$  samples for DSC measurement amounts to 20 mg.

## 3. Experimental results

The temperature dependence of IF and relative modulus of the oxide-ion conductor  $La_2Mo_2O_9$  are measured in the temperature range from 280 K to 900 K with a heating rate of  $5 \text{ K min}^{-1}$  and a vibration frequency of 1 Hz, as shown in figure 1. Two IF peaks are observed, one of them is wide and locates at about 380 K, another is sharp and centres at about 833 K. Corresponding to the low temperature peak, the modulus decreases dramatically with increase of temperature, indicating a relaxation character of this peak. This decrease of modulus is seemingly composed of two steps centred respectively at about 330 K and 390 K, implying fine structure of this peak as discussed below. Corresponding to the high temperature peak, however, the modulus exhibits a local minimum at about 840 K, a little higher than the IF peak temperature, which prompts us that the higher temperature peak was associated with a phase transition. There is also a small local minimum at about 450 K in the modulus curve, the origin of which is unclear, while no corresponding apparent changes in IF curve appear. All of the characteristics of these two peaks can be made much clearer when we measure the sample at different heating rates and different vibration frequencies.

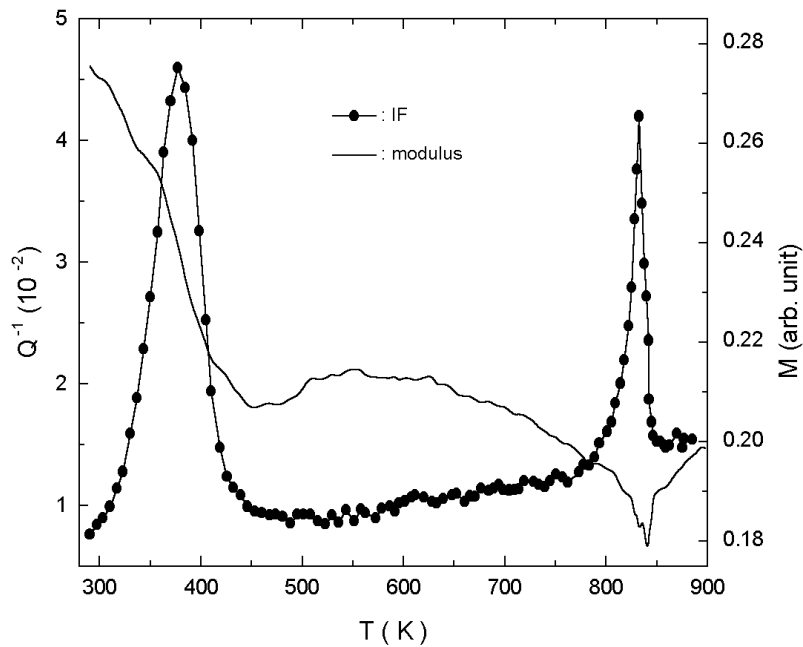


**Figure 1.** The variation of IF and relative modulus versus temperature for a  $\text{La}_2\text{Mo}_2\text{O}_9$  sample at a vibration frequency of 1 Hz and a heating rate of  $5 \text{ K min}^{-1}$ .

### 3.1. The fine structure of the low temperature relaxation peak

As a first attempt the  $Q^{-1}(T)$  curve was fitted by one Debye peak with distribution in relaxation time using a non-linear fitting method [10]. In the fitting process, we assume that the relaxation strength is independent of temperature (see results at different frequencies in the next section) and the Gaussian distribution parameter is equal to  $\beta = \beta_0 + \beta_H/kT$ , where  $\beta_0$  and  $\beta_H$  are distribution parameters of the pre-exponential factor and the activation energy in relaxation time respectively [11]. This means that the relaxation process corresponding to the IF peak is not a process of unique relaxation time, but contains a series of micro-processes with different relaxation time  $\tau$ , which continuously distributes around a most probable value  $\tau_m$  according to the Gaussian function  $\beta^{-1}\pi^{-1/2} \exp[-(z/\beta)^2]$  with  $z = \ln(\tau/\tau_m)$ . Therefore the parameter  $2\beta$  is the width of the distribution at relative height  $1/e$ . The fitting results with one Debye peak are not good enough, as shown in figure 2(a). The difference between the fitting curve and the experimental points focuses mainly on the low temperature side of the peak, which maybe indicates the existence of another IF peak at lower temperature as suggested in the above section. Thus we then fitted the  $Q^{-1}-T$  curve by two Debye peaks with distribution in relaxation time. The fitting results are shown in figure 2(b) and look satisfactory in the aspect that the fitting curve passes almost all experimental points. So it can be confirmed that the low temperature peak consists of two sub-peaks,  $P_1$  at lower temperature and  $P_2$  at higher temperature. From the fitting results, the peak temperatures at 1 Hz for  $P_1$  and  $P_2$  are 337 K and 397 K respectively. The distribution parameters for  $P_1$  and  $P_2$  are 0.13 eV and 0.08 eV for  $\beta_H$  but zero for  $\beta_0$ . The non-zero  $\beta_H$  and zero  $\beta_0$  indicate that both peaks have a distribution in activation energy but not in the pre-exponential factor of relaxation time. It is apparent that the relaxation strength of  $P_2$  is much higher than that of  $P_1$ , which is very helpful in the attempt to understand the mechanism of these peaks.

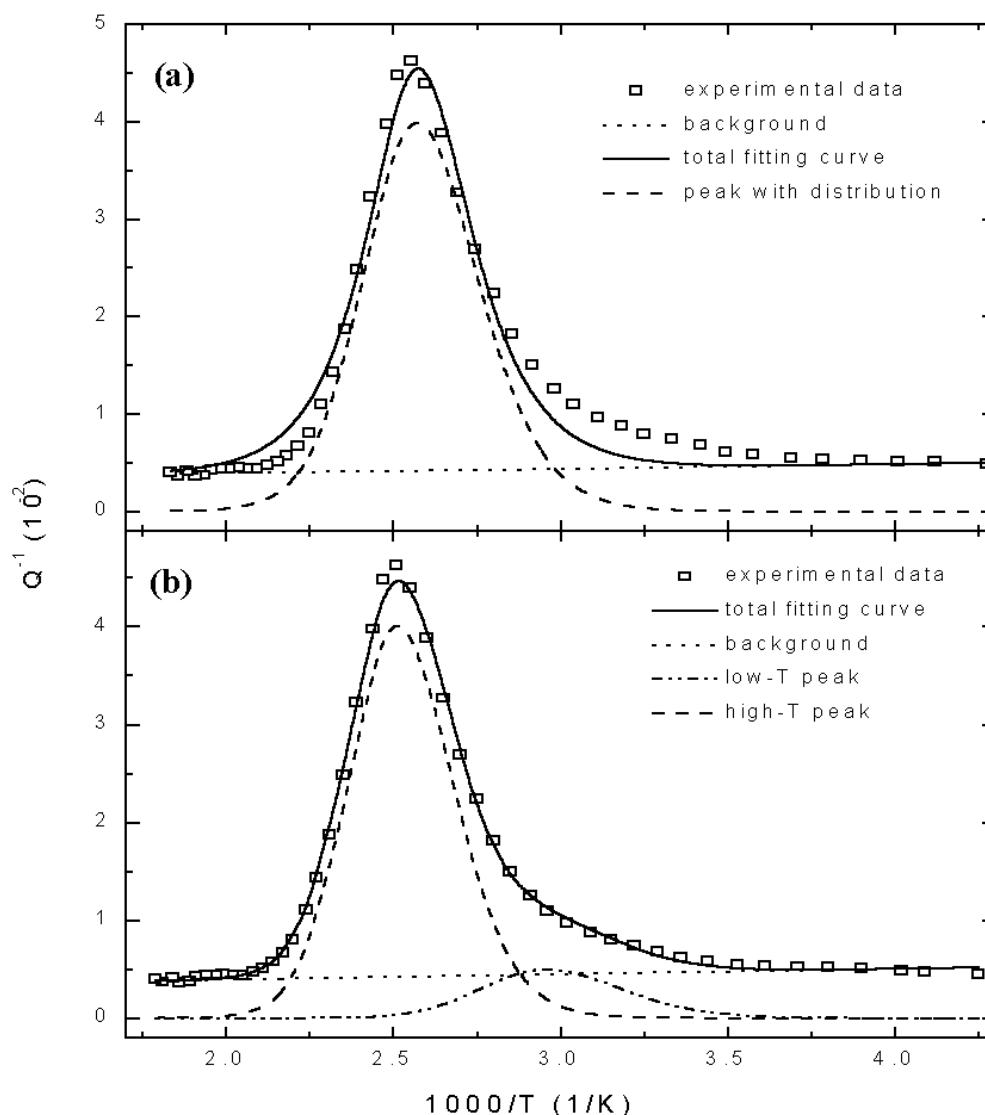


**Figure 2.** The results of non-linear fitting: (a) fitted by one Debye peak with distribution in relaxation time; (b) fitted by two Debye peaks with distribution in relaxation time. The relaxation parameters are  $\beta = 0.13$  eV/ $kT$  for the  $P_1$  peak and  $\beta = 0.08$  eV/ $kT$  for the  $P_2$  peak respectively.

### 3.2. Activation energies of the low temperature peaks

With the forced vibration method, we have simultaneously measured the IF curves of oxide-ion conductor  $\text{La}_2\text{Mo}_2\text{O}_9$  at different vibration frequencies. In figure 3 are shown the measured results at four different frequencies of 0.5, 1, 2 and 4 Hz respectively. In this figure, the symbols are experimental data points at four different frequencies, while the solid curves indicate the fitting results of the experimental data using two Debye peaks with the same distribution parameters in relaxation time as in the above section. It is clear that the peak temperature increases with the increase of vibration frequency while the relaxation strength hardly changes. For a

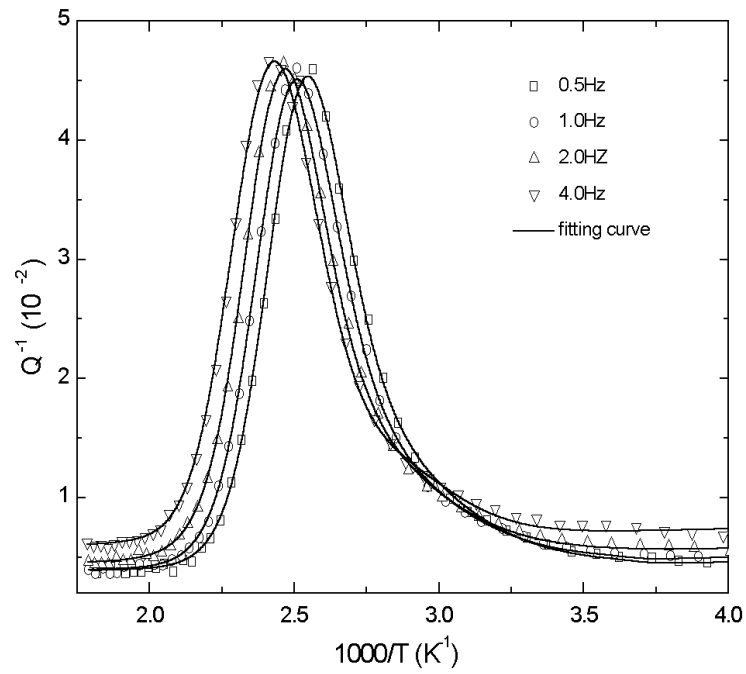


**Figure 3.** The variations of IF with temperature for a  $\text{La}_2\text{Mo}_2\text{O}_9$  sample at four different frequencies (0.5, 1.0, 2.0 and 4.0 Hz); the solid lines are the fitting results.

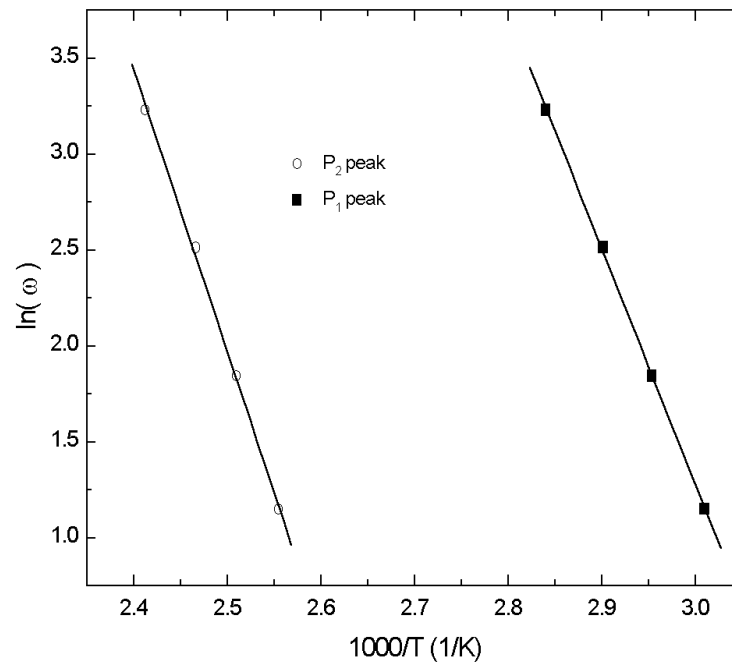


**Figure 4.** The Arrhenius plot of the two relaxation peaks ( $P_1$  and  $P_2$  peaks).

thermal relaxation peak, we have the Arrhenius relation of  $\tau = \tau_0 \exp(E/kT)$ , where  $\tau$  is the relaxation time,  $\tau_0$  is the pre-exponential factor and  $E$  is the activation energy, with the condition of  $\omega\tau = 1$  at the peak position (where  $\omega = 2\pi f$ ). If we plot the  $\ln(\omega)$  as a function of the reciprocal of peak temperature, we could deduce the parameters of  $\tau_0$  and  $E$  for both  $P_1$  and  $P_2$  peaks. The so-called Arrhenius plots for the two peaks are shown in figure 4, where the solid lines are the linear fittings. From this figure, the relaxation parameters are evaluated as  $E_1 = 1.0$  eV,  $\tau_{01} = 1.4 \times 10^{-16}$  s for the  $P_1$  peak and  $E_2 = 1.2$  eV,  $\tau_{02} = 0.8 \times 10^{-16}$  s for the  $P_2$  peak. The values of the relaxation parameters are in the same range as that for oxygen ion diffusion in oxide ceramics [7–9], suggesting a mechanism of short diffusion of oxygen ions for  $P_1$  and  $P_2$  peaks.

### 3.3. Characteristics of the high temperature peak

As for the high temperature peak, we have measured its  $Q^{-1}(T)$  curves in detail at different frequencies and different heating rates. At the same time, DSC measurements were also carried out to help discuss the mechanism of the high temperature peak.

The curves of  $Q^{-1}$  versus  $T$  obtained at 0.5 Hz by using four heating rates of 3, 5, 7 and 9 K min<sup>-1</sup> are shown in figure 5(a). It can be seen that the peak increases in height and shifts to higher temperatures when the heating rate increases, which is the typical character of the IF peaks associated with a first-order phase transition. Similarly, in the endothermal curves of DSC measurement for La<sub>2</sub>Mo<sub>2</sub>O<sub>9</sub> samples at different heating rates, the endothermal peak appears in the same temperature range, as shown in figure 5(b). The variation of this endothermal peak with heating rates is similar to the IF peak, obeying the so-called Kissinger relation [12]:

$$\ln\left(\frac{T_p^2}{\dot{T}}\right) = A + \frac{E_{ap}}{kT} \quad (1)$$

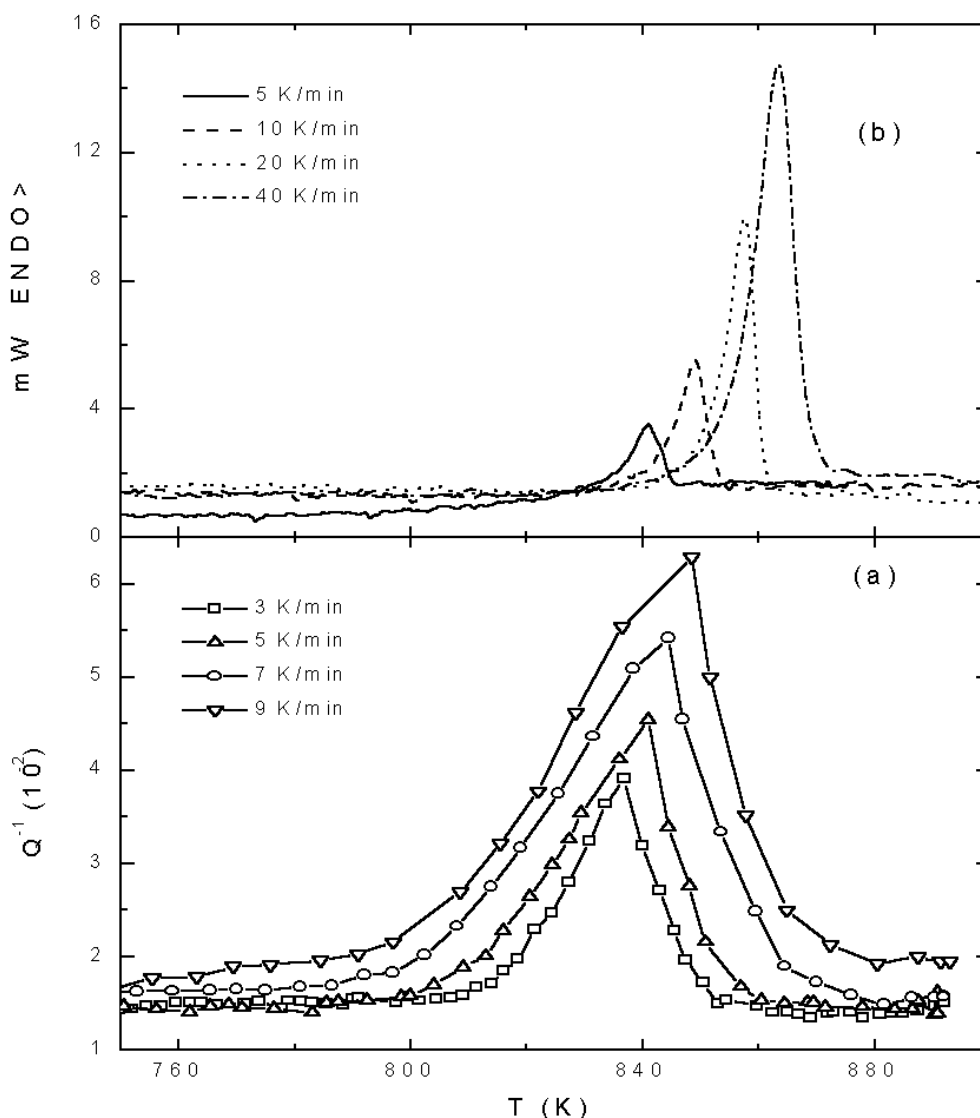
where  $A$  is a constant,  $E_{ap}$  is the apparent activation energy of the phase transition and  $k$  is the Boltzmann constant,  $T_p$  is the peak temperature and  $\dot{T}$  is the heating rate.

Figure 6 shows the curves of  $\ln(T_p^2/\dot{T})$  versus  $1/T$ . Data points from both IF and DSC measurements are well fitted into a linear line. The apparent activation energy can be obtained as  $E_{ap} = 5.3$  eV by calculating the slope of the fitting line. The fact, that the apparent activation energies obtained from IF and DSC measurements are equal to each other within the experimental error confirms the association of the high temperature peak to a first-order phase transition.

In figure 7 are shown the IF–temperature curves of the high temperature peak at different frequencies with a same heating rate of 5 K min<sup>-1</sup>, where only the results at three vibration frequencies of 0.1, 0.5 and 3 Hz are given for clarity. With the decrease of vibration frequency, the peak becomes higher but does not change its position. The peak height has a linear relation with the reciprocal of vibration frequency as shown in the inset of figure 7, which is a general character of the low frequency IF associated with the first-order phase transition. Thus we can conclude that the high temperature IF peak is associated with a structural phase transition from  $\beta$ -La<sub>2</sub>Mo<sub>2</sub>O<sub>9</sub> at high temperature to a slightly distorted phase  $\alpha$ -La<sub>2</sub>Mo<sub>2</sub>O<sub>9</sub> at low temperature.

### 3.4. Effect of Ca doping on the phase transition

Considering the improvement of low temperature conductivity of La<sub>2</sub>Mo<sub>2</sub>O<sub>9</sub>, it is very useful if the high temperature form can be stabilized to lower temperature by for example substituting the La ions with divalent ions such as Ca and Ba. We have doped La<sub>2</sub>Mo<sub>2</sub>O<sub>9</sub> samples with Ca<sup>2+</sup> ions on the La<sup>3+</sup> site with doping concentration up to 15%. The curves of IF and modulus versus temperature for the La<sub>2</sub>Mo<sub>2</sub>O<sub>9</sub> samples with three different doping concentrations (5,



**Figure 5.** (a) The curves of IF versus temperature for a  $\text{La}_2\text{Mo}_2\text{O}_9$  sample at 0.5 Hz with four different heating rates (3, 5, 7 and 9  $\text{K min}^{-1}$ ); (b) the endothermal curves of DSC at four different heating rates (5, 10, 20 and 40  $\text{K min}^{-1}$ ).

10 and 15%) are shown in figure 8, which were obtained at a vibration frequency of 1 Hz and a heating rate of 5  $\text{K min}^{-1}$ . With a 5% Ca doping, the height of the high temperature IF peak becomes 0.0043, much smaller than the value of 0.028 in the case of no Ca doping. The corresponding local minimum of the modulus also becomes smaller. When the doping content of Ca increases to 10%, the high-temperature IF peak and the local minimum of modulus disappear, indicating that the phase transition is suppressed at this Ca doping content. However the apparent change of modulus around 830 K illustrates that some structural changes still occurred in this case. When the Ca doping content reaches 15%, both IF and modulus change smoothly in the temperature range from 500 to 900 K. That is to say, doping Ca with



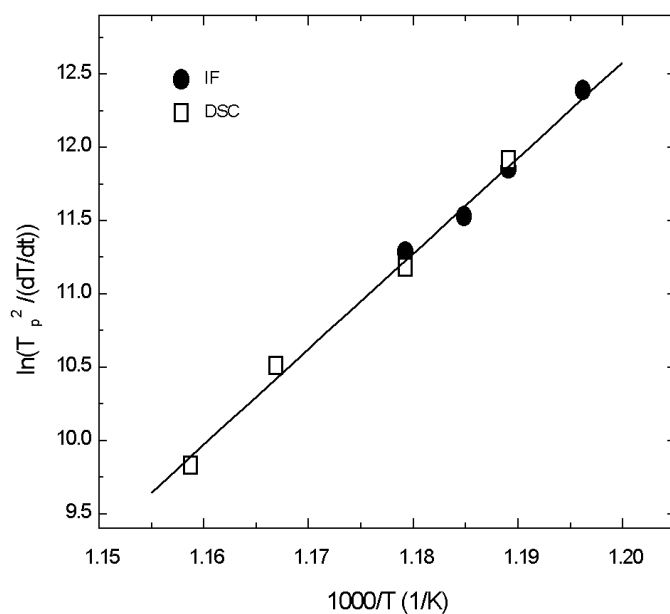


**Figure 6.** The Kissinger plot of  $\ln(T_p^2 / \dot{T})$  versus  $1/T$  for the IF and DSC measurements, giving an apparent activation energy of 5.3 eV for the phase transition.

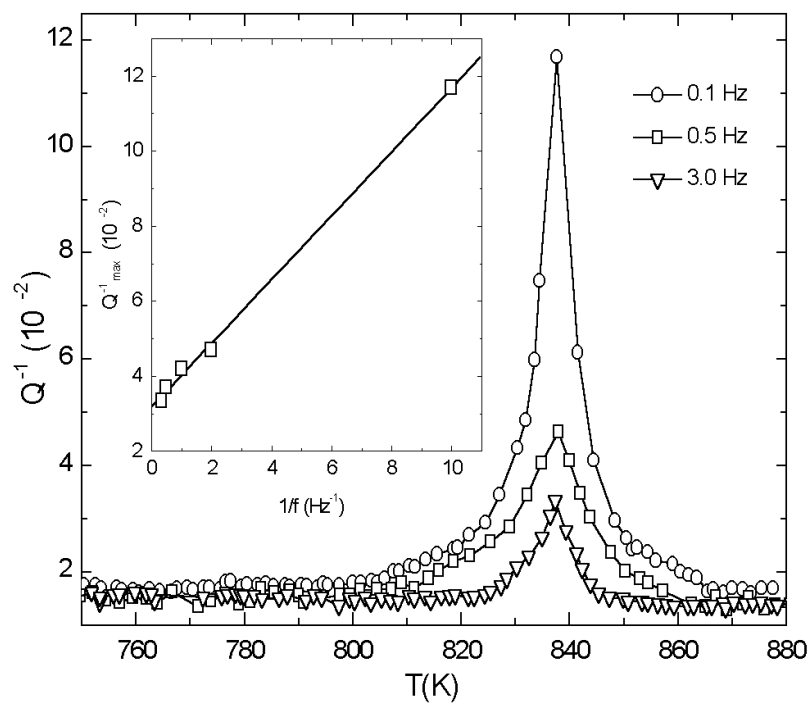


**Figure 7.** The variations of IF with ascending temperature ( $5 \text{ K min}^{-1}$ ) at three different frequencies (0.1, 0.5 and 3.0 Hz); inset: the relation between the peak height and  $1/f$ .

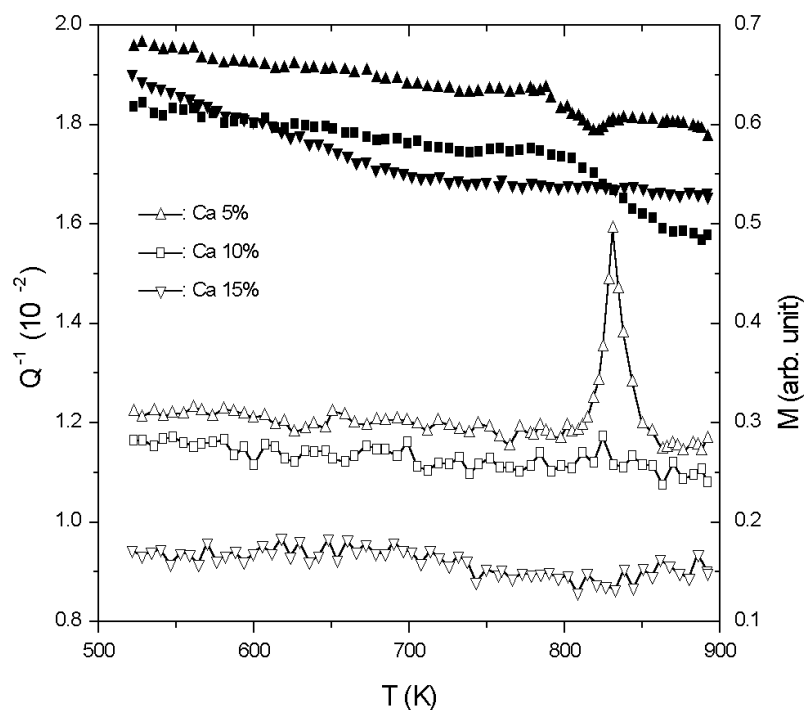


**Figure 8.** The curves of IF and relative modulus versus temperature for a  $\text{Ca}^{2+}$  doped  $\text{La}_2\text{Mo}_2\text{O}_9$  sample with three doping concentrations of 5, 10 and 15%.

15% can completely suppress the phase transition and maintain the high-temperature phase to lower temperature. In addition, it can be seen from the figure that the background IF decreases with the increase of the doping concentration.

#### 4. Discussion and conclusion

In the oxide-ion conductor  $\text{La}_2\text{Mo}_2\text{O}_9$ , high concentration of intrinsic oxygen vacancies can enhance the mobility of oxygen ions, which in turn makes the  $\text{La}_2\text{Mo}_2\text{O}_9$  a good oxide-ion conductor. As viewed from the crystal structure, both  $\beta\text{-La}_2\text{Mo}_2\text{O}_9$  and  $\beta\text{-SnWO}_4$  have the same space group of  $P213$  with identical cationic positions [5, 6]. In  $\beta\text{-SnWO}_4$ , there are two very different kinds of oxygen ion called O(1) and O(2), with the content of O(2) being much larger than that of O(1) [13]. So it is reasonable to consider that there are also two different kinds of oxygen ion in  $\text{La}_2\text{Mo}_2\text{O}_9$  and the relations between the contents of O(1) and O(2) are also similar to that in  $\text{SnWO}_4$ . In fact, x-ray and other experiments have confirmed this hypothesis [6]. Similarly in the low temperature form  $\alpha\text{-La}_2\text{Mo}_2\text{O}_9$ , there are also oxygen ions of O(1) and O(2) with a slight distortion in position relative to  $\beta\text{-La}_2\text{Mo}_2\text{O}_9$ . Because the relaxation strength is proportional to the concentration of relaxation species, the  $P_2$  peak with a much larger relaxation strength must be associated with the diffusion process of O(2) in  $\text{La}_2\text{Mo}_2\text{O}_9$ , while the  $P_1$  peak is associated with the diffusion process of O(1) via the vacancy mechanism.

Moreover, it can be seen from figure 3 that the relaxation strength does not depend on temperature. This fact indicates that the relaxation peaks originate from a disordering short-distance diffusion of oxygen ion or vacancy. This kind of phenomenon was also observed in

cuprates where the authors attributed it to disordering diffusion processes of oxygen vacancies [14, 15]. Here the word 'disordering' is used in order to distinguish from the phenomenon of stress-induced ordering diffusion. According to the point defect relaxation theory [16], the temperature dependence of the relaxation strength  $\Delta$  will be analogous to the Curie–Weiss law due to the interactions between point defects:  $\Delta \propto (T - T_c)^{-1}$ , where  $T_c$  is the critical temperature for a 'self-induced' ordering. In our case however, the relaxation strength of  $P_1$  and  $P_2$  peaks is independent of temperature and no positive (and thus meaningful)  $T_c$  exists; this means that the relaxation species (oxygen vacancies in present case) can never reach an ordering state at any temperature. In other words, the oxygen vacancies associated with  $P_1$  and  $P_2$  peaks are distributed in a disorderly way. However, to understand the mechanism of the oxygen ion or vacancy diffusion in detail, further theoretical analysis based on the crystal structure is necessary. In addition, the appearance of two relaxation peaks associated with oxygen ion diffusion indicates a complex path of oxygen ion diffusion, which supports in one aspect the hypothesis that the conductivity of oxygen ions in  $\text{La}_2\text{Mo}_2\text{O}_9$  is three dimensional in nature [6].

Lacorre *et al* have studied the structural transition of polycrystalline  $\text{La}_2\text{Mo}_2\text{O}_9$  using high-resolution x-ray thermodiffraction and found a slight structure change around 850 K [5, 6]. It was found that this structural transition played a very important role in the improvement of its conductivity, which resulted in an increase of conductivity of almost two orders of magnitude. The essential reason for this conductivity increase at high temperature originates from an order–disorder change in oxygen ion arrangement during the phase transition. In our internal friction and DSC measurements, the peak around 840 K can be ascribed to this structural transition and the difference of 10 K in transition temperature between the present and Lacorre's results may be due to the different heating rate used.

In summary, we have observed two internal friction peaks in oxide-ion conductor  $\text{La}_2\text{Mo}_2\text{O}_9$ : one is a relaxation peak and the other is associated with a first-order phase transition. The relaxation peak actually consists of two sub-peaks,  $P_1$  and  $P_2$ , which may be ascribed to the short-distance diffusion of two different kinds of oxygen ion, O(1) and O(2) in  $\text{La}_2\text{Mo}_2\text{O}_9$  samples. The difference of the relaxation strength between these two peaks originates from the difference of contents of the two oxygen ions. As for the high temperature peak, it is caused by a slight structural transition corresponding to an order–disorder change in oxygen ion arrangement. Doping with Ca ions of 15% in  $\text{La}_2\text{Mo}_2\text{O}_9$  samples can completely suppress this phase transition and maintain the high temperature phase to room temperature, which will help to improve the conducting property.

## References

- [1] Kendall K R, Navas C, Thomas J K and Loye H C Z 1995 *Solid State Ion.* **82** 215
- [2] Minh N Q 1993 *J. Am. Ceram. Soc.* **76** 563
- [3] Ishihara T, Matsuda H and Takita Y 1994 *J. Am. Chem. Soc.* **116** 3081
- [4] Kramer S A and Tuller H L 1995 *Solid State Ionics* **82** 15
- [5] Lacorre P, Goutenoire F, Bohnke O and Retoux R 2000 *Nature* **404** 856
- [6] Goutenoire F, Isnard O and Lacorre P 2000 *Chem. Mater.* **12** 2575
- [7] Weller M and Schubert H 1986 *J. Am. Ceram. Soc.* **69** 573
- [8] Rothman S J, Roubort J L and Baker J E 1989 *Phys. Rev. B* **40** 852
- [9] Matsushita K 1994 *J. Alloys Compounds* **211** 374
- [10] Yuan L X and Fang Q F 1998 *Acta Met. Sinica* **34** 1016 (in Chinese)
- [11] Nowick A S and Berry B S 1972 *Anelastic Relaxation in Crystalline Solids* (New York: Academic) pp 94–102
- [12] Kissinger H E 1957 *Anal. Chem.* **29** 1702
- [13] Jeitschko W and Sleight A W 1972 *Acta Cryst. B* **28** 3174
- [14] Zhang J X, Lin G M, Zeng W G, Liang K F, Lin Z C, Siu G G, Stokes M J and Fung P C W 1990 *Supercond. Sci. Technol.* **3** 113

- 
- [15] Zhang J X, Lin G M, Zeng W G, Liang K F, Lin Z C, Siu G G, Stokes M J and Fung P C W 1990 *Supercond. Sci. Technol.* **3** 163
- [16] Nowick A S and Berry B S 1972 *Anelastic Relaxation in Crystalline Solids* (New York: Academic) p 219